Adsorption of the liquid crystal molecule 5CB on graphene

Sean A. Fischer, Jakub Kołacz, Christopher M. Spillmann, and Daniel Gunlycke

Phys. Rev. E **98**, 052702 — Published 6 November 2018

DOI: 10.1103/PhysRevE.98.052702

Adsorption of the Liquid Crystal Molecule 5CB on Graphene

Sean A. Fischer,[1,*] Jakub Kołacz,[2] Christopher M. Spillmann,[3] and Daniel Gunlycke[1]

[1] *Chemistry Division, Naval Research Laboratory, Washington, DC 20375, United States*

[2] *ASEE Post-Doctoral Fellow at Naval Research Laboratory, Washington, DC 20375, United States*

[3] *Center for Biomolecular Science and Engineering, Naval Research Laboratory, Washington, DC 20375, United States*

(Dated: September 6, 2018)

Abstract

We use density functional theory to explore the stable adsorption geometries of the liquid crystal molecule 5CB on a graphene sheet. First, we calculate the dependence of the polarizability of 5CB on its geometry. Our results breakdown the contributions of the cyano, biphenyl, and alkyl groups to the optical properties of 5CB, confirming the biphenyl group as the most influential. Second, we quantify possible adsorption structures of 5CB on graphene. We find that 5CB can stably adsorb with its biphenyl group oriented intermediate to the armchair and zigzag crystallographic directions, in addition to adsorbing with the biphenyl oriented along those directions.

* sean.fischer@nrl.navy.mil

I. INTRODUCTION

Recently, Kim et al. proposed a fast and simple method for the direct visualization of graphene domains[1]. A liquid crystal (LC) is adsorbed on the graphene surface, and the birefringence of the system is used to determine the orientations of the domains. Beyond characterizing domains[1, 2], the method has also been used to identify defects[3, 4], edge types and chirality[5], and examine other two-dimensional materials[6, 7].

Despite the method relying on the correspondence between the orientation of the LC molecules and the graphene lattice, a detailed study of the adsorption of a LC molecule on graphene appears to be lacking. Adsorption on graphene in general is a topic that has attracted a substantial amount of attention[8–10]. Much of this work has been concerned with either the functionalization of graphene to control its properties[11] or exploring the potential of graphene as a sensor[12, 13]. In contrast, the work on LC adsorption on graphene has been concerned with either using the LC to enable characterization of the graphene[1–7] or using graphene to potentially enhance the properties of the LC[14–18]. In both cases, one of the key properties is the set of possible orientations of the LC on the graphene surface.

Surfaces are known to induce ordering in liquid crystals[19], and pioneering scanning tunneling microscopy studies observed several molecular patterns of LC on graphite[20–22]. Using graphene synthesized by chemical vapor deposition on copper foil and the LC 5CB (4'-pentyl-4-cyanobiphenyl), Yu et al. observed LC orientations separated by 30°[2]. Given the crystal structure of graphene, this separation is easy to account for by adsorption of the LC molecules along the crystallographic directions. In a subsequent study, Shehzad et al. observed LC orientations separated by only 15°[6] for 5CB on graphene exfoliated from highly oriented pyrolytic graphite and transferred to glass. This smaller separation is not as easily accounted for but is crucial to understand.

Herein we have utilized density functional theory (DFT) calculations to characterize the adsorption of the nematic LC molecule 5CB on graphene. As surfaces have been observed to induce ordering in LC, we focus on sub-monolayer coverage in the present study in order to understand the details of the interaction between the LC molecule and graphene. Our exploration of the adsorption landscape and properties of 5CB offer an explanation of the observed LC orientations. After describing the computational tools we used to probe the interactions between 5CB and graphene, we present the characterization of 5CB itself,

followed by the results for the adsorption of 5CB on graphene.

II. METHODS

Adsorption of 5CB on graphene was simulated using version 5.4 of Quantum ESPRESSO [23] with the vdW-DFT exchange-correlation functional [24–27]. The vdW-DFT functional was used as it was previously found to give the best results for aromatic adsorption on graphene[28]. We used ultrasoft pseudopotentials[29–31] generated from PSlibrary version 1.0.0[32] along with 46 and 326 Ry cutoffs for the wave functions and charge density, respectively. Our simulation cell consisted of 9x9 primitive cells of graphene and a single 5CB molecule. For our hexagonal simulation cell, $a = 22.14$ Å and $c = 20.00$ Å. The polarizability and potential energy scans of the 5CB molecule were calculated using version 6.8 of NWChem[33] with the PBE0 functional[34] and the Def2-SVP basis set[35]. The polarizability calculations were done at a excitation wavelength of 589 nm.

III. RESULTS AND DISCUSSION

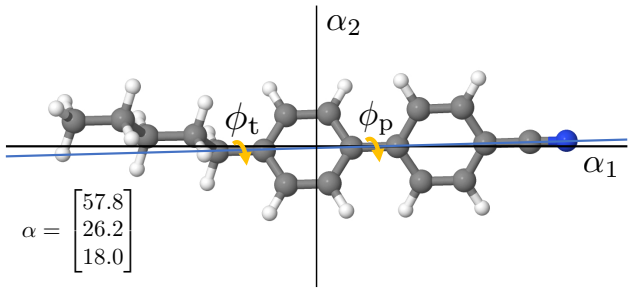

FIG. 1. LC molecule 5CB oriented in the principal axis frame of the polarizability. The angle between the major axis of the polarizability α_1 and the long axis of 5CB (blue line) is 4.05°. The principal components of the polarizability are shown in the bottom left in units of Å^3. The dihedral angle between the alkyl tail and phenyl ring is indicated by ϕ_t. The dihedral angle between the phenyl rings is indicated by ϕ_p.

A. 5CB

We begin by characterizing the 5CB molecule itself. Figure 1 shows the optimized geometry of an isolated 5CB. The dihedral angle between the alkyl tail and the neighboring phenyl ring is $\phi_t = 89.0°$, while dihedral angle between the phenyl rings is $\phi_p = 36.4°$. In its crystal structure, 5CB was found to have $\phi_t = 90.5 \pm 0.3°$ and $\phi_p = 26.3 \pm 0.3°$[36]. There is less consensus on the biphenyl dihedral angle in the LC phase, with reported values ranging from $30 \pm 2°$ to $38.4 \pm 0.1°$[37–40].

As the molecular polarizability can be related to the refractive indices[41–43], we also calculated the polarizability of 5CB at 589 nm and then aligned the molecule in the polarizability's principal axis frame (Fig. 1). The calculated isotropic polarizability $\langle\alpha\rangle$ of 34 Å^3 is in good agreement with the value of 33 Å^3 determined from experiment[42]. As can be seen in Fig. 1, the long axis of the molecule is nearly aligned with the major axis of the polarizability α_1. Specifically, the long axis of the molecule makes an angle of 4.05° with the major axis of the polarizability, where we have represented the long axis of 5CB as the unit vector pointing from the cyano carbon atom to the cyano nitrogen atom.

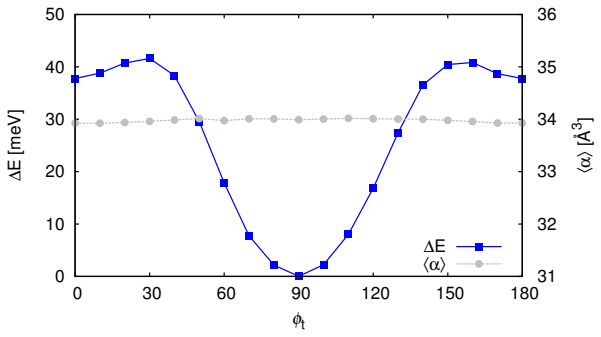

FIG. 2. Calculated potential energy and isotropic polarizability as a function of the dihedral angle between the alkyl tail and neighboring phenyl ring. The energy is given relative to the optimized ground state energy.

To gain further insight into the source of the polarizability, we calculated the isotropic polarizability for 4-pentylbiphenyl and 4-cyanobiphenyl, i.e. removing the cyano group and removing the alkyl tail, respectively. Removing the alkyl tail lowers the isotropic polarizability to 24 Å^3 from 34 Å^3. On the other hand, removing the cyano group lowers the polarizability to 30 Å^3. Combined, these results indicate that the alkyl tail contributes

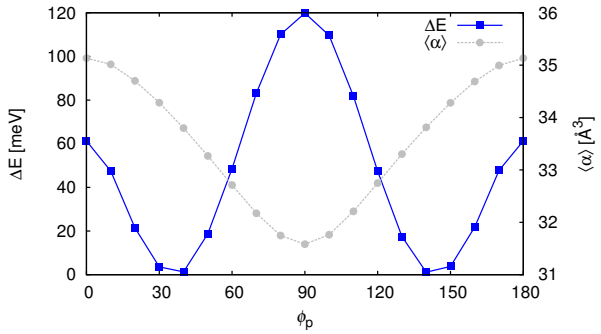

FIG. 3. Calculated potential energy and isotropic polarizability as a function of the dihedral angle between the phenyl rings. The energy is given relative to the optimized ground state energy.

29%, the biphenyl contributes 59%, and the cyano group contributes 12% to the polarizability. The small contribution of the cyano group is due to its small volume and higher electronegativity inhibiting the response of its electrons to the perturbing field.

Turning to the question of how the geometry of 5CB influences its optical properties, we calculated the isotropic polarizability of 5CB as a function of the two dihedral angles. Shown in Figs. 2 and 3 are the isotropic polarizability and potential energy as functions of ϕ_t and ϕ_p, respectively. There is reasonable freedom in the orientation of the alkyl tail with respect to the biphenyl group as the barrier to rotation is comparable to thermal energy ($k_BT = 26$ meV, at 298 K). At the same time, ϕ_p has a more limited range as the associated barriers are much larger. Of course, these are the barriers for a gas-phase molecule, the corresponding barriers in the LC phase are likely to be larger due to intermolecular interactions and steric hinderance.

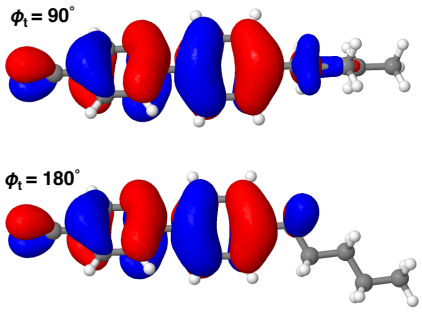

FIG. 4. Highest occupied molecular orbitals when the alkyl tail is oriented 90° and 180° relative to the neighboring phenyl ring. The two colors represent the phases of the orbitals.

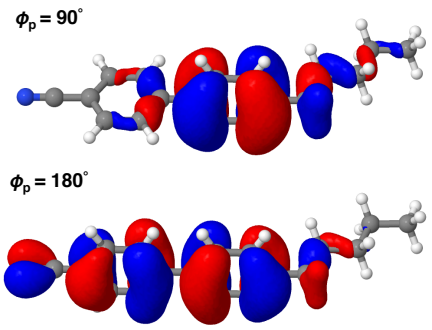

FIG. 5. Highest occupied molecular orbitals when the biphenyl dihedral is 90° and 180°. The two colors represent the phases of the orbitals.

Comparing the calculated isotropic polarizability as a function of ϕ_t and ϕ_p, it is clear that the relative orientation of the phenyl rings would be expected to have a much larger effect on the optical properties than would the orientation of the alkyl tail relative to the biphenyl group. This behavior can be understood by looking at the highest occupied molecular orbitals (HOMOs) for different configurations. Figure 4 shows the HOMO for when $\phi_t = 90°$ and $\phi_t = 180°$. The electron density is delocalized across the biphenyl and cyano groups for both tail orientations, with the classic π-bonding seen for the aromatic rings. This contrasts with the HOMO for when $\phi_p = 90°$ and $\phi_p = 180°$ as shown in Fig. 5. Here there is good delocalization when the rings are planar, but when the rings are perpendicular to each other, the electron density becomes localized on just one of the rings. This localization will constrain the response of those electrons to an electric field, resulting in a lower polarizability.

B. 5CB on Graphene

Our study of the polarizability of 5CB makes clear that different orientations of 5CB on graphene must correspond to different orientations of the biphenyl, in contrast to the previous suggestion that the additional orientations could be attributed to the position of the alkyl tail relative to the biphenyl[6]. Given that various moiré patterns have been observed with bilayer graphene and with graphite[44–49], it is reasonable to assume that there could be stable adsorption geometries of 5CB beyond those lying along the crystallographic directions. Indeed this is precisely what we found; there exists an additional stable adsorption geometry

that lies in between the expected armchair and zigzag orientations.

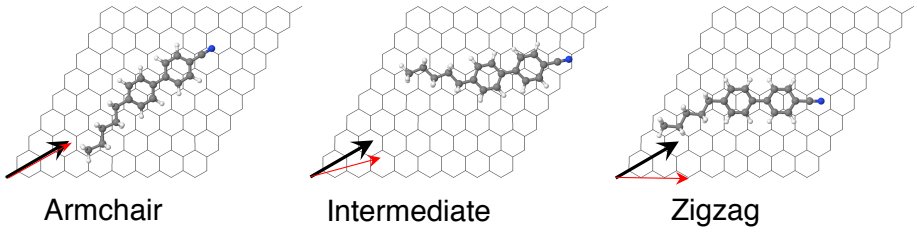

FIG. 6. Lowest-energy structures for each adsorption orientation. The graphene sheets have been rendered as wireframes for clarity. The thick, black arrow represents the armchair direction of graphene, while the thinner, red arrow indicates the average orientations. The angles θ between these lines are given in Table I.

Figure 6 shows the lowest-energy structures that we found for each orientation. In addition to these structures, we identified 9 other adsorption geometries for each orientation. All 30 structures appear to be thermally accessible as they are within $\sim$ 40 meV of each other[50]. In particular, we point out that adsorption along the armchair direction gives the familiar AB or Bernal stacking of the aromatic rings, and while this stacking pattern is stable, the current level of theory gives the structure in Fig. 6 as lower in energy by $\sim$ 4 meV.

For characterizing the adsorption orientations, we have averaged over the 10 structures found for each orientation, with each structure weighted by its Boltzmann relative probability

$$p_i = \frac{e^{-\epsilon_i/k_B T}}{\sum_{j=1}^{M} e^{-\epsilon_j/k_B T}} \tag{1}$$

where ϵ_i is the electronic energy of the i-th structure, T is taken as 298.15 K, and M is the total number of structures. We have assumed that entropic factors for each adsorption geometry would be similar and therefore can be left out. Additionally, we have assumed that each structure would have a similar excitation spectrum, and therefore considering only the lowest energy electronic configuration is sufficient for relative populations.

In Table I we have collected some relevant descriptors of the three orientations. Because all of the calculated structures are similar in energy, Boltzmann statistics predicts that all would be significantly populated. Though we are simulating sub-monolayer coverage, the

relatively even distribution of populations is consistent with recent experimental observations performed with a bulk LC layer[6]. The single most stable adsorption orientation was found along the armchair direction; although, there were adsorption structures for the other orientations very close in energy to the lowest energy one, thereby keeping us from making a definitive statement concerning the lowest energy orientation[50]. On average there is almost no difference in binding energy amongst the three orientations as seen in Table I.

As in Fig 1, we quantified the orientation of 5CB by taking the unit vector pointing from the cyano carbon atom to the cyano nitrogen atom as the molecule's long axis. The angle θ between this axis and the armchair direction of graphene determines the molecular orientation on the surface. As can be seen in Table I, the average separation between orientations is $15.16 \pm 1.59°$, which is in good agreement with the $15 \pm 1°$ separations between director orientations seen experimentally[6]. We note that while we concluded that the position of the alkyl tail alone was insufficient to account for the additional orientations that were observed experimentally, here we did find that the position of the alkyl tail can have a small impact on individual adsorption orientations[50]. When these small deviations among the individual structures are averaged together, the experimental trend is recovered.

TABLE I. Summary of adsorption parameters. The relative populations are based on Boltzmann statistics and the total electronic energies. The binding energies have been calculated according to $E_B = E_{5CB::G} - E_{5CB} - E_G$. Orientation refers to the angle that the cyano group of 5CB makes with the armchair direction of the graphene surface. This was calculated by an orthogonal projection of the carbon-nitrogen bond vector into the xy plane. The distance of 5CB from the surface is averaged over all atoms of the 5CB molecule

	Armchair	Intermediate	Zigzag
Relative population	0.348	0.325	0.326
Binding energy	-1.472 eV	-1.475 eV	-1.472 eV
Orientation (θ)	1.52°	15.55°	31.83°
Distance from surface	3.68 Å	3.67 Å	3.73 Å
Biphenyl dihedral (ϕ_{p})	13.45°	12.17°	22.78°

The distance between 5CB and graphene is approximately two times the van der Waals radius of carbon[51], which is consistent with the adsorption being due to van der Waals

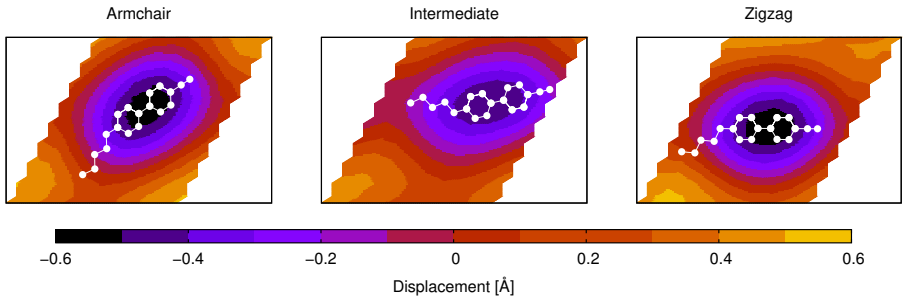

FIG. 7. Out-of-plane displacement for the carbon atoms of graphene. The heavy atoms of the adsorbed 5CB molecule are indicated by the white circles.

forces. When adsorbed along the zigzag direction, 5CB sits slightly further away on average and its phenyl rings have a slightly larger dihedral angle. In all cases though, ϕ_{p} is smaller than for the isolated molecule. Given the dependence of the polarizability on ϕ_{p} (Fig. 3), this could indicate that graphene has the potential to increase the optical properties of the LC. Of course, there would have to be a long coherence length for the LC such that the changes in molecular geometry induced by the surface are propagated up into the bulk LC phase.

For each orientation, we found that adsorption of 5CB results in significant distortion of the graphene sheet. This is illustrated in Fig. 7. While the carbon atoms of graphene move very little within the plane from their pristine locations, the displacement out-of-plane is substantial. For all adsorption structures, the carbon atoms below 5CB move up to 0.6 Å below the original plane of graphene while the other carbon atoms move up to 0.6 Å above the original plane. It is unclear whether the deformation of graphene would have any observable impact on the properties of the system or whether the deformation would persist in the presence of a substrate or a bulk layer of LC.

To test whether our results depend sensitively on the deformation of graphene, which presumably could be restricted if the graphene were over a substrate rather than in free space, we re-optimized 5 structures for each orientation with the graphene atoms constrained to remain in the original plane. Note, the graphene carbon atoms were free to move within the plane. Table II presents the descriptors for these constrained calculations. While there are small changes to the relative populations, binding energies, and geometric parameters, the overall picture remains the same. Note, that the relative orientations do not appear

to agree as well with experiment for the constrained graphene sheet, but that is because this subset of structures only sampled one tail position for each orientation. Including the complementary tail positions for each structure would result in the average orientations aligning better with the experimental results.

TABLE II. Summary of adsorption parameters for constrained graphene. The relative populations are based on Boltzmann statistics and the total electronic energies. The binding energies have been calculated according to $E_B = E_{5CB::G} - E_{5CB} - E_G$. Orientation refers to the angle that the cyano group of 5CB makes with the armchair direction of the graphene surface. This was calculated by an orthogonal projection of the carbon-nitrogen bond vector into the xy plane. The distance of 5CB from the surface is averaged over all atoms of the 5CB molecule

	Armchair	Intermediate	Zigzag
Relative population	0.415	0.327	0.399
Binding energy	-1.375 eV	-1.367 eV	-1.375 eV
Orientation (θ)	2.96°	11.70°	29.13°
Distance from surface	3.67 Å	3.66 Å	3.73 Å
Biphenyl dihedral (ϕ_{p})	14.78°	11.09°	24.26°

IV. CONCLUSIONS

We showed that in addition to the expected adsorption of 5CB along the armchair and zigzag directions of graphene, there exists an additional, stable adsorption orientation intermediate to these two. It is this intermediate adsorption structure that seems likely as the origin of the additional orientations observed previously[6]; although, extrapolation from sub-monolayer coverage to bulk LC is not necessarily straightforward and will be investigated further in the future. For a single molecule adsorbing on graphene, we found a multitude of low energy structures, though all falling into one of the three orientation categories. In addition, we have demonstrated that, as expected, the unique optical properties of 5CB are mostly due to the biphenyl group. Furthermore, we detailed how the polarizability of 5CB depends on the geometric parameters of the molecule. Future studies will examine how the findings presented here are modulated by intermolecular interactions between 5CB

molecules.

CONFLICTS OF INTEREST

There are no conflicts to declare.

ACKNOWLEDGMENTS

The authors acknowledge support from the U.S. Office of Naval Research directly and through the U.S. Naval Research Laboratory.

---

[1] D. W. Kim, Y. H. Kim, H. S. Jeong, and H.-T. Jung, Nat. Nanotechnol. **7**, 29 (2012).

[2] J.-S. Yu, X. Jin, J. Park, D. H. Kim, D.-H. Ha, D.-H. Chae, W.-S. Kim, C. Hwang, and J.-H. Kim, Carbon **76**, 113 (2014).

[3] J.-H. Son, S.-J. Baeck, M.-H. Park, J.-B. Lee, C.-W. Yang, J.-K. Song, W.-C. Zin, and J.-H. Ahn, Nat. Commun. **5**, 3484 (2014).

[4] Y. J. Lim, B. H. Lee, Y. R. Kwon, Y. E. Choi, G. Murali, J. H. Lee, V. L. Nguyen, Y. H. Lee, and S. H. Lee, Opt. Express **23**, 14162 (2015).

[5] J.-S. Yu, D.-H. Ha, and J.-H. Kim, Nanotechnology **23**, 395704 (2012).

[6] M. A. Shehzad, D. H. Tien, M. W. Iqbal, J. Eom, J. H. Park, C. Hwang, and Y. Seo, Sci. Rep. **5**, 13331 (2015).

[7] M. A. Shehzad, S. Hussain, J. Lee, J. Jung, N. Lee, G. Kim, and Y. Seo, Nano Lett. **17**, 1474 (2017).

[8] L. Kong, A. Enders, T. S. Rahman, and P. A. Dowben, J. Phys.: Condens. Matter **26**, 443001 (2014).

[9] P. Lazar, F. Karlický, P. Jurečka, M. Kocman, E. Otyepková, K. Šafářová, and M. Otyepka, J. Am. Chem. Soc. **135**, 6372 (2013).

[10] L. Chen, E. E. L. Tanner, and R. G. Compton, Phys. Chem. Chem. Phys. **19**, 17521 (2017).

[11] V. Georgakilas, M. Otyepka, A. B. Bourlinos, V. Chandra, N. Kim, K. C. Kemp, P. Hobza, R. Zboril, and K. S. Kim, Chem. Rev. **112**, 6156 (2012).

[12] F. Schedin, A. K. Geim, S. V. Morozov, E. W. Hill, P. Blake, M. I. Katsnelson, and K. S. Novoselov, Nat. Mater. **6**, 652 (2007).

[13] S. Myung, P. T. Yin, C. Kim, J. Park, A. Solanki, P. I. Reyes, Y. Lu, K. S. Kim, and K.-B. Lee, Adv. Mater. **24**, 6081 (2012).

[14] R. Basu and S. A. Shalov, Phys. Rev. E **96**, 012702 (2017).

[15] R. Basu, A. Garvey, and D. Kinnamon, J. Appl. Phys. **117**, 074301 (2015).

[16] R. Basu, D. Kinnamon, and A. Garvey, Liq. Cryst. **43**, 2375 (2016).

[17] R. Basu, D. Kinnamon, and A. Garvey, Appl. Phys. Lett. **106**, 201909 (2015).

[18] R. Basu, Phys. Rev. E **96**, 012707 (2017).

[19] B. Jerome, Rep. Prog. Phys. **54**, 391 (1991).

[20] J. S. Foster and J. E. Frommer, Nature **333**, 542 (1988).

[21] D. P. E. Smith, H. Hörber, C. Gerber, and G. Binnig, Science **245**, 43 (1989).

[22] M. Shigeno, W. Mizutani, M. Suginoya, M. Ohmi, K. Kajimura, and M. Ono, Jpn. J. Appl. Phys. **29**, L119 (1990).

[23] P. Giannozzi, S. Baroni, N. Bonini, M. Calandra, R. Car, C. Cavazzoni, D. Ceresoli, G. L. Chiarotti, M. Cococcioni, I. Dabo, A. Dal Corso, S. de Gironcoli, S. Fabris, G. Fratesi, R. Gebauer, U. Gerstmann, C. Gougoussis, A. Kokalj, M. Lazzeri, L. Martin-Samos, N. Marzari, F. Mauri, R. Mazzarello, S. Paolini, A. Pasquarello, L. Paulatto, C. Sbraccia, S. Scandolo, G. Sclauzero, A. P. Seitsonen, A. Smogunov, P. Umari, and R. M. Wentzcovitch, J. Phys.: Condens. Matter **21**, 395502 (2009).

[24] T. Thonhauser, S. Zuluaga, C. A. Arter, K. Berland, E. Schröder, and P. Hyldgaard, Phys. Rev. Lett. **115**, 136402 (2015).

[25] T. Thonhauser, V. R. Cooper, S. Li, A. Puzder, P. Hyldgaard, and D. C. Langreth, Phys. Rev. B **76**, 125112 (2007).

[26] K. Berland, V. R. Cooper, K. Lee, E. Schröder, T. Thonhauser, P. Hyldgaard, and B. I. Lundqvist, Rep. Prog. Phys. **78**, 066501 (2015).

[27] D. C. Langreth, B. I. Lundqvist, S. D. Chakarova-Käck, V. R. Cooper, M. Dion, P. Hyldgaard, A. Kelkkanen, J. Kleis, L. Kong, S. Li, P. G. Moses, E. Murray, A. Puzder, H. Rydberg, E. Schröder, and T. Thonhauser, J. Phys.: Condens. Matter **21**, 084203 (2009).

[28] J. Björk, F. Hanke, C.-A. Palma, P. Samori, M. Cecchini, and M. Persson, J. Phys. Chem. Lett. **1**, 3407 (2010).

[29] D. Vanderbilt, Phys. Rev. B **41**, 7892 (1990).

[30] K. Laasonen, R. Car, C. Lee, and D. Vanderbilt, Phys. Rev. B **43**, 6796 (1991).

[31] K. Laasonen, A. Pasquarello, R. Car, C. Lee, and D. Vanderbilt, Phys. Rev. B **47**, 10142 (1993).

[32] A. Dal Corso, Comp. Mater. Sci. **95**, 337 (2014).

[33] M. Valiev, E. J. Bylaska, N. Govind, K. Kowalski, T. P. Straatsma, H. J. J. Van Dam, D. Wang, J. Nieplocha, E. Aprà, T. L. Windus, and W. A. de Jong, Comput. Phys. Commun. **181**, 1477 (2010).

[34] C. Adamo and V. Barone, J. Chem. Phys. **110**, 6158 (1999).

[35] F. Weigend and R. Ahlrichs, Phys. Chem. Chem. Phys. **7**, 3297 (2005).

[36] T. Hanemann, W. Haase, I. Svoboda, and H. Fuess, Liq. Cryst. **19**, 699 (1995).

[37] S. Sinton and A. Pines, Chem. Phys. Lett. **76**, 263 (1980).

[38] S. W. Sinton, D. B. Zax, J. B. Murdoch, and A. Pines, Mol. Phys. **53**, 333 (1984).

[39] G. Celebre, M. Longeri, E. Sicilia, and J. W. Emsley, Liq. Cryst. **7**, 731 (1990).

[40] D. Sandström and M. H. Levitt, J. Am. Chem. Soc. **118**, 6966 (1996).

[41] J. Li and S.-T. Wu, J. Appl. Phys. **95**, 896 (2004).

[42] J. Li and S.-T. Wu, J. Appl. Phys. **96**, 6253 (2004).

[43] J. S.-P., S.-C. Huang, K.-H. Lin, H.-Y. Chen, and T.-K. Shen, J. Phys. Chem. C **120**, 14277 (2016).

[44] G. Li, A. Luican, J. M. B. Lopes dos Santos, A. H. Castro Neto, A. Reina, J. Kong, and E. Y. Andrei, Nat. Phys. **6**, 109 (2010).

[45] G. Trambly de Laissardière, D. Mayou, and L. Magaud, Nano Lett. **10**, 804 (2010).

[46] R. Bistritzer and A. H. MacDonald, P. Natl. Acad. Sci. USA **108**, 12233 (2011).

[47] Z. Y. Rong and P. Kuiper, Phys. Rev. B **48**, 17427 (1993).

[48] J. Xhie, K. Sattler, M. Ge, and N. Venkateswaran, Phys. Rev. B **47**, 15835 (1993).

[49] M. Kuwabara, D. R. Clarke, and D. A. Smith, Appl. Phys. Lett. **56**, 2396 (1990).

[50] See Supplemental Material at [] for all optimized structures and calculated properties.

[51] S. S. Batsanov, Inorg. Mater.+ **37**, 871 (2001).